SIMULATING GAS EXCHANGE IN THE HUMAN LUNG AND BODY

Noah D. Syroid, Joseph A. Orr, Dwayne R. Westenskow

Departments of Bioengineering and Anesthesiology
The University of Utah
Salt Lake City, UT 84132

Abstract

We have implemented a real-time simulator of gas-exchange in the human body and lung. The system realistically mimics respiratory gas uptake and production as a function of pulmonary, cardiovascular, and metabolic parameters. The implementation consists of hardware and software to control the flow of gases entering and leaving a ventilated test lung. Such a device could serve as a bench-top resource for testing newly developed anesthesia, hemodynamic, and patient monitors. Preliminary tests have been performed for validation of a non-invasive cardiac monitor. The results, while promising, expose the need for more sophisticated models of the human respiratory and circulatory physiology.

Introduction

Modeling and simulation are important means of testing and validating new medical devices without involving live subjects. Human and animal testing is expensive and might pose logistical, ethical and political challenges. Furthermore, control of parameters may be difficult or impossible to obtain during an experiment on live subjects. While modeling and simulation does not replace in *vivo* testing, it may aid in validating new instrumentation with less cost, less development time, and equal accuracy.

With this in mind, we have created a human lung simulator to validate prototype anesthesia instrumentation. The simulator design and implementation may be described on three basic levels: hardware to control gas flow through an artificial lung, software to control the hardware, and software to simulate gas exchange in the human body's tissues and lungs.

Hardware

Figure 1 shows a schematic of the simulator's physical components. Since the largest portion of ambient air is composed of N_2, O_2, and CO_2, we use three mass flow controllers (MFCs) [Porter Instrument Co. Inc.] to regulate the flow of these gases from pressurized tanks into a ventilated test/training lung (TTL). A fan inside the TTL provides active mixing of the gases from the lung

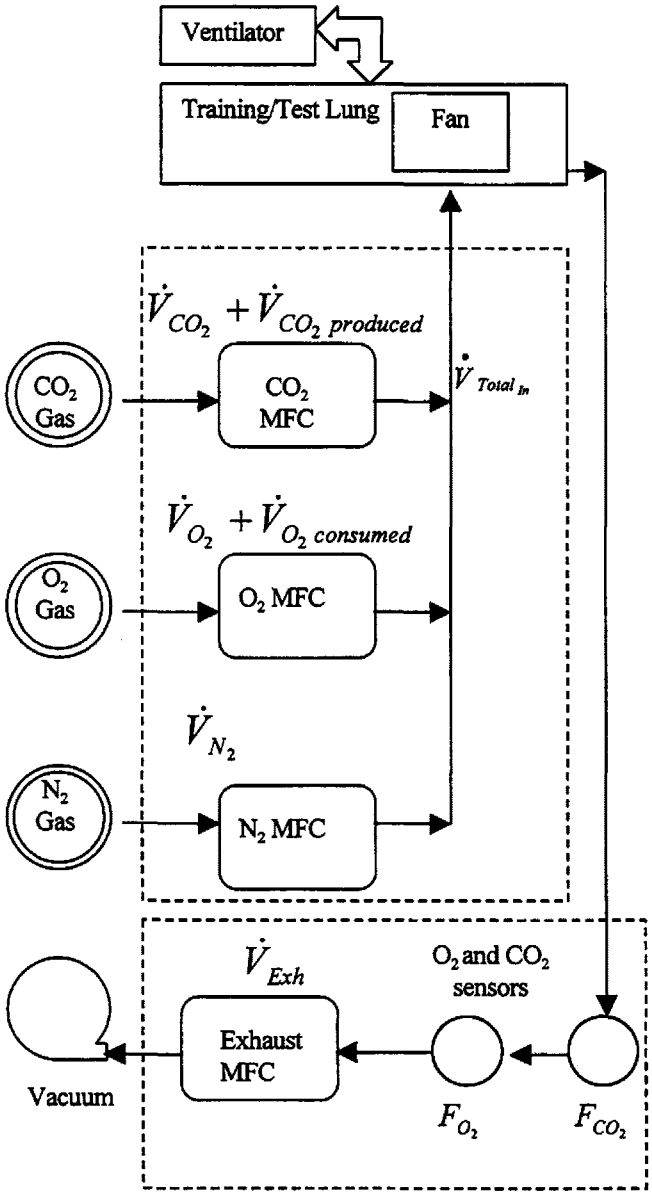

Figure 1: Physical Components of the Lung Simulator

simulator and the ventilator. A vacuum is used to pull the mixed gas from the TTL in which the flow is regulated by the exhaust MFC. O_2 and CO_2 sensors, located in the exhaust flow, record the concentrations of oxygen and carbon dioxide in the lung. A microprocessor controls the flow of the MFCs and receives input from the O_2 sensors.

A personal computer communicates with the microprocessor and provides the user with an interface to input various physiologic parameters (see Figure 2).

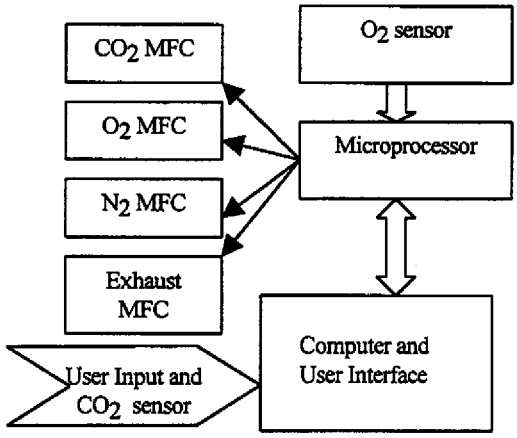

Figure 2: Microprocessor Control and Communication

Software to Control the Hardware

The O_2 and CO_2 sensors are used to calculate the flow of oxygen $(\dot{V}_{O_2})$, carbon dioxide $(\dot{V}_{CO_2})$, and nitrogen $(\dot{V}_{N_2})$ pulled from the lung by the vacuum. The exhaust flow $(\dot{V}_{Exh})$ is set at a constant rate, so

$$\dot{V}_{O_2} = \dot{V}_{Exh} \cdot F_{O_2}, \text{ (liters/min)} \quad (1)$$

and

$$\dot{V}_{CO_2} = \dot{V}_{Exh} \cdot F_{CO_2} \text{ (liters/min)}, \quad (2)$$

where F_{O_2} and F_{CO_2} is the fraction of O_2 and CO_2 measured by the sensors in the exhaust flow. Also,

$$\dot{V}_{Exh} = \dot{V}_{CO_2} + \dot{V}_{O_2} + \dot{V}_{N_2} = const. \text{ (liters/min)}, \quad (3)$$

and we may solve for N_2 flow to and from the lung:

$$\dot{V}_{N_2} = \dot{V}_{Exh} - (\dot{V}_{CO_2} + \dot{V}_{O_2}) \text{ (liters/min)}. \quad (4)$$

Using equations (1) – (4), we may define the flow of gas into the lung, $\dot{V}_{Total_{In}}$:

$$\dot{V}_{Total_{In}} = \overbrace{\left[\dot{V}_{CO_2} + \dot{V}_{CO_2 produced}\right]}^{CO_2 MFC Flow} + \overbrace{\left[\dot{V}_{O_2} - \dot{V}_{O_2 consumed}\right]}^{O_2 MFC Flow} + \overbrace{\dot{V}_{N_2}}^{N_2 MFC Flow} \quad (5)$$

The parameters $\dot{V}_{O_2 consumed}$ and $\dot{V}_{CO_2 produced}$ in Figure 1 and Equation (5) represent the production of CO_2 and consumption of O_2 in the body. In steady state, these values also represent the net flow of CO_2 and O_2 exchanged across the lung wall. How these values are computed is explained in a later section.

Gas Exchange Physiology

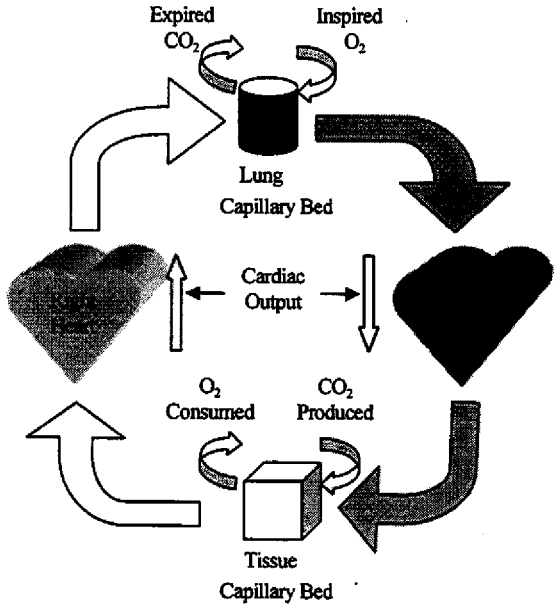

Figure 3: Circulation and Gas Exchange in the Human Body and Lung

Figure 3 demonstrates O_2 consumption, CO_2 production, and blood flow on an elementary level. O_2 is inspired into the alveoli of the lungs where it diffuses across the alveolar membrane and pulmonary capillary membrane. Likewise, CO_2 diffuses from the blood in the pulmonary capillary beds and into the alveoli. Oxygen rich blood is pumped by the left heart into the tissue capillary bed. In the tissues, metabolism consumes O_2 and produces CO_2, and diffusion occurs from the tissues to the capillaries. Thus, CO_2 rich blood is pumped through the right side of the heart and back into the lung [1]. Many processes affect the exchange of oxygen and carbon dioxide including cardiac output, O_2/CO_2 diffusion,

ventilation, perfusion, metabolism, and pH.

Cardiac Output, Ventilation, Perfusion, and Metabolism

Cardiac output is related to gas exchange using a mass balance equation, also known as the Fick principle (assuming steady state) [2]:

$$\dot{Q} = \frac{\dot{V}_{co_2\ produced}}{c_{\bar{v}_{co_2}} - c_{a_{co_2}}}, \qquad (6)$$

where $\dot{Q}$ is cardiac output (liters/minute), $\dot{V}_{co_2\ produced}$ is the amount of CO2 produced by tissue metabolism, (liters/minute), $c_{\bar{v}_{co_2}}$ is the mixed venous CO_2 concentration of the blood (blood flowing into lungs in % volume) and $c_{a_{co_2}}$ is the arterial CO_2 concentration of blood flowing from the lungs (% volume). The same equation holds for oxygen consumption with an opposite sign for the arterial-venous gradient:

$$\dot{Q} = \frac{\dot{V}_{o_2\ consumed}}{c_{a_{o_2}} - c_{\bar{v}_{o_2}}}. \qquad (7)$$

Figure 3 and Equations (6) and (7) assume that $\dot{Q}$ also represents blood flow through the pulmonary capillaries. Unfortunately some blood bypasses the lung (shunt). Some fraction of shunt is attributed to normal processes. For instance, cardiac blood flow in the Thebesian veins naturally shunt blood. Some pulmonary disorders also increase shunt. That is, a disorder may cause some of the blood flowing through the pulmonary capillaries to not perfuse or exchange gas with the alveoli, and compromise the efficiency of the lung [2].

Gas exchange is also dependent on alveolar ventilation, $\dot{V}_A$, a value that represents how much "fresh gas" suitable for gas exchange reach the alveoli. The trachea and unperfused alveoli are unable participate in gas exchange but contribute to the volume of the lung. This volume is called dead space, V_D. The volume of atmospheric gas inhaled and exhaled for each breath (tidal volume, V_T) must exceed the amount of dead space for exchange with "fresh" gas to occur. Equation (8) exemplifies this:

$$\dot{V}_A = (V_T - V_D) \cdot RR, \qquad (8)$$

where RR is the respiratory rate in breaths per minute [1].

CO_2 and O_2 are the basic products and sources of metabolism. Thus, $\dot{V}_{co_2\ produced}$ and $\dot{V}_{o_2\ consumed}$ are also indicative of metabolism, and their ratio,

$$R = \frac{\dot{V}_{CO_2\ produced}}{\dot{V}_{O_2\ consumed}}, \qquad (9)$$

is a measure of oxidation of fats, carbohydrates and proteins. Typically, $R_{fat} = 0.7$, $R_{carbohydrate} = 1.0$, and $R_{protein} = 0.8$. For a healthy human, a typical steady state value for R is 0.8.

O_2 and CO_2 Diffusion

Oxygen flow $(\dot{V}_{O_2})$ from the alveoli into the capillaries is driven passively by diffusion. The Bohr equation relates O_2 flow to the partial pressure of the alveoli $(P_{A_{O_2}})$ and the mean pulmonary capillary blood partial pressure $(P_{pcb_{O_2}})$, where

$$\dot{V}_{O_2} = \frac{K \cdot A \cdot (P_{A_{O_2}} - P_{pcb_{O_2}})}{L} \text{ [3,4].} \qquad (10)$$

The parameters K, A, and L, respectively convey the diffusion coefficient, alveolar surface area, and path length for diffusion. The $P_{A_{O_2}} - P_{pcb_{O_2}}$ gradient is the driving pressure for diffusion, but $P_{pcb_{O_2}}$ also depends on the process of O_2 chemically binding with hemoglobin [3].

Diffusion of O_2 from the alveoli and into the pulmonary capillary red blood cells (RBCs) occurs across three membranes. First, there is the alveolar-capillary tissue barrier of variable thickness consisting of endothelial and epithelial cells. Second, there is the plasma barrier, the fluid between the membrane and the RBC. Finally, there is the plasma/RBC barrier where oxygen must travel from the plasma into the interior of the RBC to bind with the hemoglobin [4]. There are four heme units per hemoglobin molecule (an amino-acid peptide protein), where each heme unit contains an iron atom capable of bonding (non-covalently) to an oxygen molecule [1].

CO_2 exchange from the pulmonary capillary bed to the alveoli of the lung occurs more readily than O_2 exchange. The rate at which CO_2 may diffuse is approximately 20 times higher than O_2 [2]. Typically, the

diffusion gradient is adequate such that arterial and alveolar CO_2 are equilibrated in steady state,

$$P_{a_{CO_2}} \cong P_{A_{CO_2}}. \quad (11)$$

Blood Acid-Base Balance

The human body has the ability to store CO_2, which serves as a pH buffer system. Body pH is regulated tightly as enzymatic activities may occur in the pH range of 6.8 to 7.8 [3]. Most CO_2 is transported through the blood as bicarbonate, and the buffering system may be described in terms of a chemical reaction:

$$CO_2 + H_2O \xleftrightarrow{slow} H_2CO_3 \leftrightarrow HCO_3^- + H^+ \text{ [1]}. \quad (12)$$

The pH of the body may be related to P_{CO_2} by the Henderson-Hasselbach equation:

$$pH = pK + \log\left(\frac{[HCO_3^-]}{\alpha \cdot P_{CO_2}}\right), \quad (13)$$

where pK is the apparent dissociation constant, and α is a solubility constant [1,3]. P_{CO_2} is sensed in the cerebral spinal fluid and controlled by ventilation.

CO_2 and O_2 Dissociation Curves

It is convenient to examine O_2 and CO_2 levels in the lung as a partial pressure (P_{O_2}, P_{CO_2}, mm Hg) and in the body as a concentration (c_{O_2}, c_{CO_2}, ml/l of blood). Thus, a relation is required between P and c, and this is achieved though a dissociation curve. Capek and Roy empirically derived such a curve as shown in Figure 4 [5]. Additional dissociation curves by Chiari et al.[6], Grodins et al. [7], and Loeppky et al. [8] have been formulated using acid-base and empirical models yield similar results. The dissociation curve not only relies on CO_2, but also relies on O_2. A decrease in oxygen saturation or P_{O_2} will shift the curve up and left. This shift is called the Haldane effect [3,6].

The concentration of O_2 in the blood is the amount of oxygen bound to hemoglobin together with the amount of O_2 dissolved in blood. Therefore, one may relate the arterial blood oxygen concentration to partial pressure:

$$C_{a_{O_2}} = [HbO_2] \cdot CC_{Hb} \cdot S_{O_2} + \beta \cdot P_{a_{O_2}} \text{ (\% vol)}. \quad (14)$$

Here, $[HbO_2]$ is the concentration of oxyhemoglobin (oxygen-bound hemoglobin), CC_{Hb} is the O_2 carrying capacity of hemoglobin (ml O2/g Hb), So_2 is percent of oxygen saturated hemoglobin, and β is the solubility of oxygen in blood plasma [2].

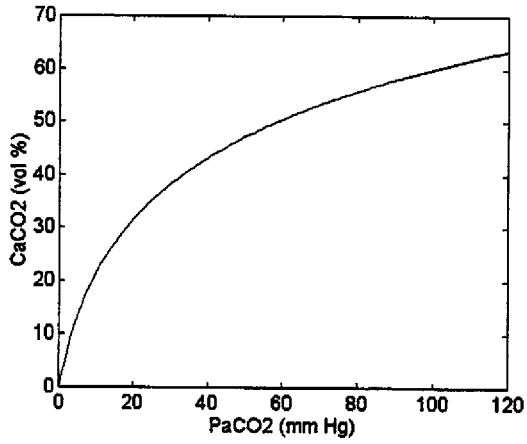

Figure 4 : Capek and Roy CO_2 Dissociation Curve With Hb = 15 g/dl

Gas Exchange and Circulation Models

Using physiology as a basis, models may be formulated to varying complexities to simulate gas exchange and blood circulation in the human body.

Fick Equation to Model CO_2 Gas Exchange

The Fick equation, Equation (6), was used as a model to simulate CO_2 production given a cardiac output value. This model was conducive for use with our simulator. If $\dot{Q}$ is given and $c_{\bar{v}_{co_2}}$ is constant, Equation (6) may be rearranged so that:

$$\dot{V}_{co_2\ produced} = \dot{Q} \cdot (c_{\bar{v}_{co_2}} - c_{a_{co_2}}) \quad (15)$$

Since the simulator measures the CO_2 fraction of the gas in the lung, then

$$P_{a_{co_2}} = F_{CO_2} \cdot P_{barometric} \text{ (mm Hg)}, \quad (16)$$

and $c_{a_{co_2}}$ may be obtained from a dissociation curve such as the one shown in Figure 4.

Preliminary simulator tests were performed with a non-invasive cardiac output monitor [NICO, Novametrix Inc.] that used partial rebreathing and a differential form of Equation (6). This device had been validated against the

thermodilution method of measuring cardiac output in several animal studies [9]. The goal was to observe how well the simulator's parameters matched the monitor's computed and measured parameters and to see how cardiac output of the simulator compared with the monitor's cardiac output value.

Figure 5 shows the results of one such preliminary test. The set cardiac output of the simulator (thin solid line) was ramped from 2 l/min to 6 l/min over a period of two hours. The thick solid line represents the monitor's estimate of pulmonary capillary blood flow (PCBF). The figure shows good correlation at low to medium PCBF values. At high PCBF values, the monitor's values overestimated the simulator's set values. It was observed that small oscillations in the CO_2 signal caused large, quick changes in gas flow.

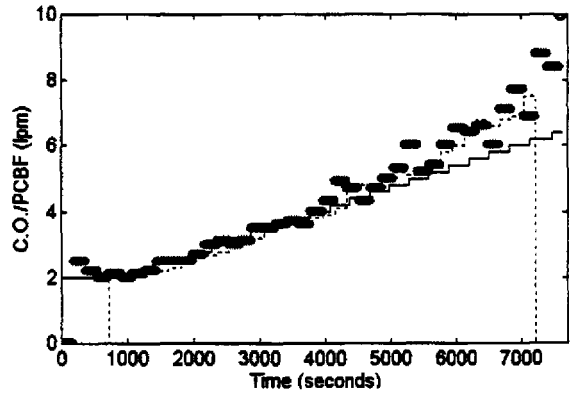

Figure 5: PCBF Values Between the Simulator (Set, Thin Solid Line) and the Non-invasive Cardiac Output Monitor (Measured, Thick Line).

It seemed that the MFCs became unstable at high cardiac outputs, and this caused the observed over-estimations. The inaccuracy is believed to be due to a delay between the time at which a gas flow was set and the time at which the gas flow had reached the set point. As shown in Figure 6, it takes the MFC approximately 2 seconds for actual flow to equilibrate with set flow [10]. The steady-state properties of the Fick equation and the MFC delays caused the simulator system to become unstable at high cardiac outputs. The large set cardiac output values drove the CO_2 MFC via Equation (16) to produce a large flow range for CO_2. The delay in the CO_2 MFC would then cause a time where CO_2 flow was too high. The system in turn would then drive the MFC to produce little or no flow. The response to this action was delayed, and the result was unstable cycling of the CO_2 signal.

The constant mixed venous CO_2 concentration used

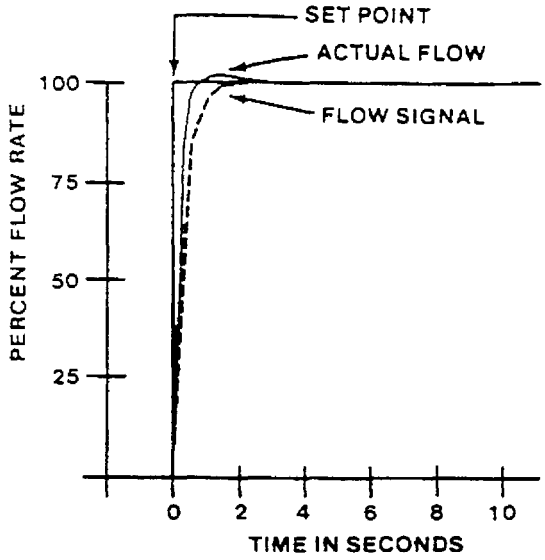

Figure 6 Mass Flow Controller Step Response[10]

by the simulator does not allow appropriate simulation for blood recirculation. For instance, the non-invasive cardiac monitor used in the preliminary tests artificially elevates inspired CO_2 levels transiently by increasing the dead space of the patient's breathing apparatus. This results in a temporary increase in arterial blood CO_2 levels. Normally, small transient changes in $Paco_2$ will not be reflected on the venous side. The body's ability to maintain large stores of CO_2 effectively low pass filters the perturbation. However, a long-term elevation of $Paco_2$, or certain physiologic conditions may cause an increase in the mixed venous blood [9].

Oxygen Consumption

In order to simulate oxygen exchange accurately, a faster oxygen sensor is required for the simulator. Figure 7 shows the step response for a change in the simulator's set O_2 concentration from 20% to 90%. A time of nearly 60 seconds is required for the simulator's measured concentration to equilibrate with the set concentration. While some delay is the result of mixing in the lung volume, most of the delay is attributed to the response time of the sensor. The slight overestimate of the measured O_2 signal at steady-state was due to a calibration error.

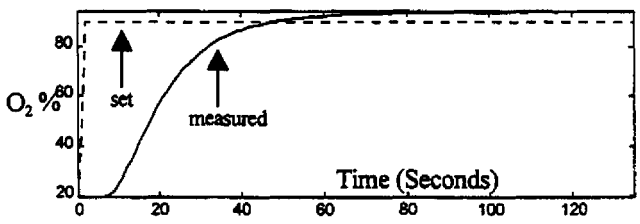

Figure 7: Step Response of Simulator O_2 %

In the past, oxygen consumption has not been the

focus of research for the simulator. Typically constant flows of O_2 have sufficed for device testing. For research on sophisticated gas exchange and circulation models, O_2 consumption will certainly be a concern. At this point, it would be necessary to find a more responsive O_2 sensor. Faster, more expensive, sensors are available, and when it is deemed necessary, the appropriate modifications to the simulator will be made.

Extensive Models for Gas Exchange and Circulation

The Fick model is a specific solution to relate respiratory exchange to cardiac output. A general model would be desirable for the simulator in order to test a spectrum of monitoring products. Chari et al.., have developed such a model by using non-linear differential equations to represent circulation and gas exchange [6]. The equations are presented below, and they are generalized. That is, there are two sets of equations for O_2 and CO_2 for each equation below. First, the lung processes may be defined in terms of mass balance:

$$V_A \frac{dP_A}{dt} = \dot{V} \cdot (P_I - P_A) + \lambda \cdot \dot{Q} \cdot (1-s) \cdot (C_v - C_e). \quad (17)$$

Note that *(1-s)* represents the non-shunted blood to the pulmonary capillary beds. P_I represents the partial pressure of the inspired gas, C_e is the end pulmonary gas concentration and λ is the dissociation function that converts concentrations to partial pressure. The concentrations entering and bypassing the lung illustrate the shunt equation:

$$C_a = (1-s) \cdot C_e + s \cdot C_v. \quad (18)$$

Mass balance in the brain is defined as

$$V_B \frac{dC_B}{dt} = \dot{Q}_B \cdot (C_a - C_{vb}) + MP_B, \quad (19)$$

where MP_B describes the rate of CO_2/O_2 metabolic production/consumption in the brain, and C_{vb} is the venous concentration after gas exchange in the brain. The same may be done for the tissues:

$$V_T \frac{dC_T}{dt} = \dot{Q}_T \cdot (C_a - C_{vt}) + MP_T. \quad (20)$$

Again, C_{vt} is the mixed venous concentration in the tissues, and MP_T is the metabolic production rate in the tissues. Finally, the blood flow may be related to the blood gas concentrations:

$$C_V = \frac{\dot{Q}_T}{\dot{Q}} \cdot C_{vt} + \frac{\dot{Q}_B}{\dot{Q}} \cdot C_{vt}, \; \dot{Q} = \dot{Q}_T + \dot{Q}_B \text{ [6]}. \quad (21)$$

Chari et al.. also describe a system of equations for respiratory control and the dissociation curve function λ [6]. For a mechanically ventilated simulator, it is not necessary to provide a model for respiratory control. That is, our simulator assumes that a patient is anesthetized and mechanically ventilated. Hill et al.. have also proposed similar exchange and circulatory models, but their models are derived from models describing diffusion of a gas across the alveolar-capillary membrane, empirically measured circulatory times, and a model for acid-base balance [11].

An implementation would be achieved by performing numerical integration using a third order Runge Kutta algorithm [12]. The differential equations would be solved for O_2 consumption and CO_2 production, and these values would be substituted in Equation (5). The models above would also serve as a basis for more detailed simulation. For instance, Equation (18)'s value for the shunt *s* is constant. Additional models that simulated shunt could be implemented and tested. The resulting design leads to a base circulation and exchange model with a hierarchy of "plug-in" models that may be implemented as needed.

Discussion

A real-time simulator was implemented to provide a means for testing respiratory and patient monitors. Software controlled hardware regulates gas flow into a mechanically ventilated lung. Software models simulate gas exchange and circulation in the human lung and body.

The Fick model was used to perform preliminary tests on a non-invasive cardiac output monitor, and to provide some information on the simulator's accuracy, utility, and shortcomings. The results from the preliminary tests suggested improvements to the hardware and software of the system.

Acknowledgements

Many thanks to Dr. Orr, Dr. Westenskow, Kai Kuck, and Volker Boehm for help on implementation of the simulator and models. Thanks to Novametrix Inc. for use of their monitoring devices, firmware, and software.

References

[1] Rhoades R, Pflanzer R. Human Physiology: Saunders College Publishing. 1996.

[2] Hlastala MP, Berger AJ. Physiology of Respiration. Oxford University Press. 1996.

[3] Berne RM, Levy MN. Physiology. Mosby Year Book. 1993.

[4] Weibel ER. *Lung Mophometry and Models in Respiratory Physiology.* Chapter from: Respiratory Physiology: An Analytical Approach. 40:1-56, 1989.

[5] Capek JM. Roy RJ. Noninvasive measurement of cardiac output using partial CO_2 rebreathing. *IEEE Transactions on Biomedical Engineering.* 25(9):653-61. 1988.

[6] Chiari L, Avanzolini G, Ursino M. A comprehensive simulator of the human respiratory system: validation with experimental and simulated data. *Annals of Biomedical Engineering.* 25:985-99, 1997.

[7] Grodins FS, Buell J, Bart AJ. Mathematical analysis and digital simulation of the respiratory control system. *Journal of Applied Physiology.* 22:260-76, 1967.

[8] Loeppky JA, Luft UC, Fletcher ER. Quantitative description of whole blood CO_2 dissociation curve and Haldane effect. *Respiratory Physiology.* 51:167-81, 1983.

[9] Haryadi DG, Orr, JA, Kück, K. McJames, S, Westenskow, DR. Evaluation of a partial CO2 rebreathing Fick technique for measurement of cardiac output, *Anesthesiology*, 1998, 89(3a), A534.

[10] Figure Adapted From: Fast Response Mass Flowmeter and Controller Series 100F and 200F Technical and Users Manual. Porter Instrument Co. Inc. 4.4, 1982.

[11] Hill EP, Power CG, Longo LD. *Kineteics of O_2 and CO_2 Gas Exchange.* Chapter from: West JB. Ed. Bioengineering Aspects of the Lung. 3:459-514, 1977.

[12] Press WH, Teukolsky SA. Vetterling WT. Flannery BP. Numerical Recipes in C, 2nd Editon. Cambridge University Press. 710-14, 1994.